

## Spin-State Equilibria in Holmium Cobaltate

V. G. Bhide, D. S. Rajoria, and Y. S. Reddy  
National Physical Laboratory, New Delhi 110012, India

G. Rama Rao and C. N. R. Rao

Department of Chemistry, Indian Institute of Technology, Kanpur-20a016, India

(Received 14 March 1973; revised manuscript received 26 June 1973)

Mössbauer and magnetic susceptibility studies of  $\text{HoCoO}_3$  have shown that there is coexistence of low-spin  $\text{Co(III)}$  ions and high-spin  $\text{Co}^{3+}$  ions;  $\text{Co(III)}$  being more predominant at low temperatures. The population of  $\text{Co(III)}$  and  $\text{Co}^{3+}$  equalizes above a particular temperature with these ions occupying alternate oxygen octahedra, leading to an ordered phase. The ordering transition is evidenced by the temperature variation of Lamb-Mössbauer factor, x-ray Debye-Waller factor, and inverse susceptibility. Electrical-conductivity data reflect these changes in the spin-state equilibria and show that at around 1080 K,  $\text{HoCoO}_3$  becomes metallic. At this temperature, a first-order localized electron-collective electron transition seems to occur.  $\text{Co(II)}$  and  $\text{Co}^{4+}$  are not formed by electron transfer from  $\text{Co}^{3+}$  to  $\text{Co(III)}$  as in  $\text{LaCoO}_3$ . This behavior is correlated with the variation of covalency in the cobaltates.

### I. INTRODUCTION

Rare-earth perovskites  $\text{La}^{+3}\text{B}^{+3}\text{O}_3$  ( $B$  is a transition-metal atom) have been investigated in great detail in recent years.<sup>1-3</sup> The  $d$  electrons of the transition-metal ions in these perovskites are localized or itinerant depending on the valence and the spin state of the transition-metal ion. Thus,  $\text{LaNiO}_3$  and  $\text{LaTiO}_3$  ( $s = \frac{1}{2}$ ) have collective  $d$  electrons and are metallic.<sup>1,2</sup> On the other hand,  $\text{LaCrO}_3$ ,  $\text{LaMnO}_3$ , and  $\text{LaFeO}_3$  with high-spin transition-metal ions exhibit localized behavior of  $d$  electrons.<sup>1,2,4</sup>

The rare-earth perovskite  $\text{LaCoO}_3$  shows the presence of both high-spin and low-spin trivalent cobalt ions and a well-defined first-order transition from localized- to itinerant-electron behavior at 1210 K.<sup>5</sup> The high-spin-low-spin equilibria in  $\text{LaCoO}_3$  were recently investigated by us in detail employing Mössbauer spectroscopy along with magnetic susceptibility and other measurements.<sup>6</sup> These studies show that the cobalt ion in  $\text{LaCoO}_3$  exists predominantly in the low-spin  $\text{Co(III)}$  state at low temperatures and partially transforms to high-spin  $\text{Co}^{3+}$  state up to 200 K. Above 200 K,  $\text{Co(II)}$  and  $\text{Co}^{4+}$  ions are formed by the transfer of  $d$  electrons from  $\text{Co}^{3+}$  to  $\text{Co(III)}$ ;  $\text{Co}^{3+}$  ions completely disappear at the localized-to-itinerant-electron transition temperature. The changes in spin equilibria are also reflected in the electron-transport properties of  $\text{LaCoO}_3$ . These studies have enabled us to clarify the nature of the spin-state equilibria and the phase transition which are in essential accord with the mechanism of Raccach and Goodenough.<sup>5</sup> Studies on  $\text{NdCoO}_3$  and  $\text{GdCoO}_3$  have also shown properties similar to  $\text{LaCoO}_3$ .<sup>7</sup>

An interesting aspect in our study of  $\text{LaCoO}_3$  was the apparent difference between the nature of the spin equilibrium of the cobalt ions shown by mag-

netic-susceptibility data and Mössbauer studies.<sup>6</sup> Magnetic-susceptibility data also show that, at low temperatures, cobalt ions exist predominantly in the low-spin state and transform to high-spin  $\text{Co}^{3+}$  partially up to  $\sim 200$  K. The relation between the  $\text{Co}^{3+}$ -to- $\text{Co(III)}$  ratio and the susceptibility is given by

$$\text{Co}^{3+}/\text{Co(III)} = \frac{1}{N^2 \mu^2 / 3R\chi_g T - 1}, \quad (1)$$

where  $\mu$  is the spin-only moment of  $\text{Co}^{3+}$  ions. A plot of  $\chi_g T$  against temperature of  $\text{LaCoO}_3$  showed a significantly different behavior above 200 K from that obtained for the proportion of high-spin  $\text{Co}^{3+}$  from Mössbauer spectra. This was explained as follows.<sup>6,7</sup> At low temperatures, Mössbauer spectra consist of two resonances, one due to the low-spin  $\text{Co(III)}$  and the other due to the high-spin  $\text{Co}^{3+}$ . However, electron transfer from  $\text{Co}^{3+}$  to  $\text{Co(III)}$  above 200 K gives rise to spin states [ $\text{Co(II)}$  and  $\text{Co}^{4+}$ ] which are paramagnetic, but exhibit isomer shifts which overlap the resonance due to the low-spin  $\text{Co(III)}$ . While this mechanism explained the observed differences between the magnetic susceptibility and Mössbauer data, there was no definitive proof for the mechanism.

We have presently investigated the spin equilibria in  $\text{HoCoO}_3$  employing magnetic susceptibility and Mössbauer studies. This study shows that the cobalt ions are predominantly low-spin  $\text{Co(III)}$  up to a particular temperature above which there is a sudden change in the relative proportion of  $\text{Co(III)}$  and  $\text{Co}^{3+}$  ions. The  $\text{Co}^{3+}$  and  $\text{Co(III)}$  ions become equally populated in this high-temperature region and occupy alternate oxygen octahedra giving rise to long-range order. The isomer shift, the Lamb-Mössbauer factor, as well as the x-ray Debye-Waller factor clearly bring out this transition. It is indeed interesting that the same relative propor-

tion of the spin states is obtained from both Mössbauer spectroscopy and magnetic-susceptibility measurements in this cobaltate. This correspondence between the two measurements in  $\text{HoCoO}_3$  justifies our earlier assumption<sup>6,7</sup> that  $\text{Co}^{3+}$  and  $\text{Co(III)}$  ions produce  $\text{Fe}^{3+}$  and  $\text{Fe(III)}$ , respectively, on electron capture and that electron-transfer from  $\text{Co}^{3+}$  to  $\text{Co(III)}$  (producing different states of cobalt) in  $\text{LaCoO}_3$  is responsible for the apparent difference between the  $\text{Co}^{3+}$  population from Mössbauer and  $\chi_g T$  data. Electron-transport properties of  $\text{HoCoO}_3$  are also found to reflect the spin-state equilibria.

## II. EXPERIMENTAL

$\text{HoCoO}_3$  was prepared by the decomposition of holmium cobalticyanide as suggested by Gallagher.<sup>8</sup> The cobalticyanide decomposes to the cobaltate completely at around 920 K which is stable up to 1200 K as evidenced by thermogravimetric analysis. Above 1200 K, there appears to be some evidence of decomposition. We made two samples of  $\text{HoCoO}_3$  by the cobalticyanide method, one by heating the cobalticyanide around 1190 K for 15 h (sample I) and the other around 980 K for 5 h (sample II).

Differential thermal analysis (DTA) was done using an Aminco differential thermal analyzer. The lattice parameters of  $\text{HoCoO}_3$  were determined at different temperatures in the range 300–1100 K employing a General Electric XRD-6 diffractometer fitted with a furnace assembly. X-ray Debye-Waller factors were calculated employing the diffractometer profiles. The magnetic susceptibility of  $\text{HoCoO}_3$  was measured by the Gouy technique over the temperature range 78–1200 K. The electrical resistivity of  $\text{HoCoO}_3$  was measured in the 180–1210-K range on pressed pellets sintered (at 980 or 1190 K) employing the four-probe technique. Seebeck coefficients relative to platinum were measured in the range 400–1240 K.

For Mössbauer-effect studies,  $\text{HoCoO}_3$  was used as a source. While preparing the Mössbauer source, two different methods were followed. In one of them,  $\text{Co}^{57}$  was doped into the corresponding compounds before thermal decomposition leading to  $\text{HoCoO}_3$ . In the other, a few drops of aqueous solution of  $\text{Co}^{57}\text{Cl}_2$  were dropped on the disc of  $\text{HoCoO}_3$ ;  $\text{Co}^{57}$  was thermally diffused in  $\text{HoCoO}_3$  around 1000 K for 4 h. After thermal diffusion of  $\text{Co}^{57}$ , the sample was slowly cooled to room temperature. Both these sources gave identical results. These sources were matched against enriched  $\text{Na}_4\text{Fe(CN)}_6 \cdot 10\text{H}_2\text{O}$  single-crystal absorbers. The Lamb-Mössbauer factor at various temperatures was determined using a black absorber. Mössbauer spectra were recorded on a mechanical drive spectrometer described earlier.<sup>9</sup>

The investigations were carried out in detail on

sample I and crucial experiments were repeated with sample II as well.

## III. RESULTS AND DISCUSSION

Figure 1 shows a typical Mössbauer spectra obtained using  $\text{HoCoO}_3$  as a source over the temperature range 78–800 K. These spectra are characterized by two resonances which are almost equally intense above 300 K, but with different intensities below 200 K. At room temperature, these two resonances are located at  $0.20 \pm 0.04$  and  $0.57 \pm 0.04$  mm/sec. It is tempting to attribute these two resonances to the two partners of a quadrupole split spectrum. However, little consideration will show that they arise because of the existence of two distinct valence states.<sup>6,7</sup> In this lattice, quadrupole interaction is expected to be negligible. Further, the center of gravity of the two resonances does not correspond to any of the valence states and in the low-temperature region, the two resonances are not equally intense. From the isomer-shift systematics, the high-energy resonance appears to arise out of  $\text{Fe}^{3+}$ , whereas the lower-energy resonance seems to be due to  $\text{Fe(III)}$ . The intensities of the two resonances were determined from the row dips (depth of the resonances) as well as from the area under the resonances. Implicit in the above is the assumption that the Debye-Waller factors for both the states are identical. It will be seen that below 300 K,  $\text{Fe(III)}$  is more intense than the  $\text{Fe}^{3+}$  state. Above 300 K, however, both the states seem to be populated with equal intensity. Based on arguments presented earlier,<sup>6,7</sup> we would expect the low-spin  $\text{Co(III)}$  to give low-spin  $\text{Fe(III)}$  on electron capture and that high-spin  $\text{Co}^{3+}$  to give high-spin  $\text{Fe}^{3+}$ . Thus the ratio  $\text{Fe}^{3+}/\text{Fe(III)}$  from the Mössbauer spectra should reflect the ratio of  $\text{Co}^{3+}/\text{Co(III)}$  in  $\text{HoCoO}_3$ .

Magnetic-susceptibility measurements provide a further check on the above inference. Figure 2(a) shows the inverse magnetic susceptibility  $1/\chi_g$  as a function of temperature. This curve is marked by two linear regions with slightly different slopes separated by a flat portion extending over a temperature region 250–350 K. It is possible to determine the effective magnetic moments in the two linear temperature regions. We see that in the lower-temperature region, the effective magnetic moment<sup>10</sup> is  $10.3\mu_B$ , whereas in the higher-temperature region, the effective magnetic moment is  $14.53\mu_B$ . These results clearly show that as the temperature increases, the magnetic character of the substance is changing. This may be due to the conversion of low-spin diamagnetic  $\text{Co(III)}$  to high-spin paramagnetic  $\text{Co}^{3+}$ . Indeed a similar susceptibility variation characterized by a plateau separating the two linear regions has been observed in  $\text{MnAs}_{1-x}\text{P}_x$  and  $\text{LaCoO}_3$  and has been interpreted on

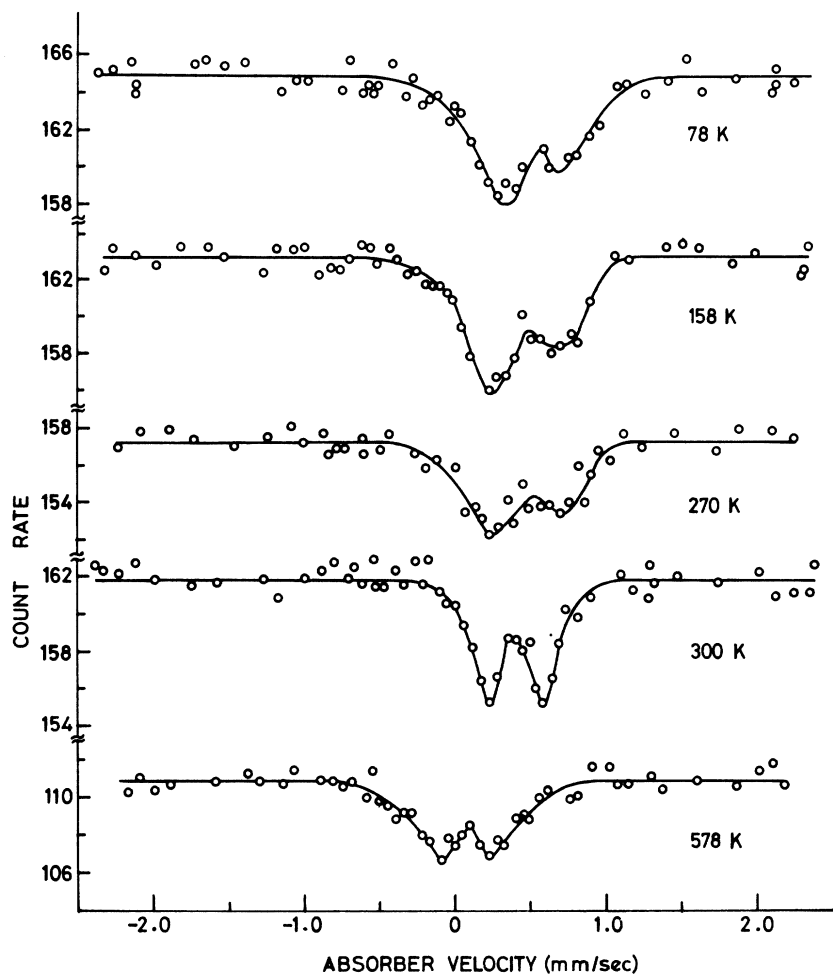


FIG. 1. Typical spectra of  $\text{HoCoO}_3 : \text{Co}^{57}$  (sample I) matched against  $\text{NaFe}(\text{CN})_6 \cdot 10\text{H}_2\text{O}$  single-crystal absorber.

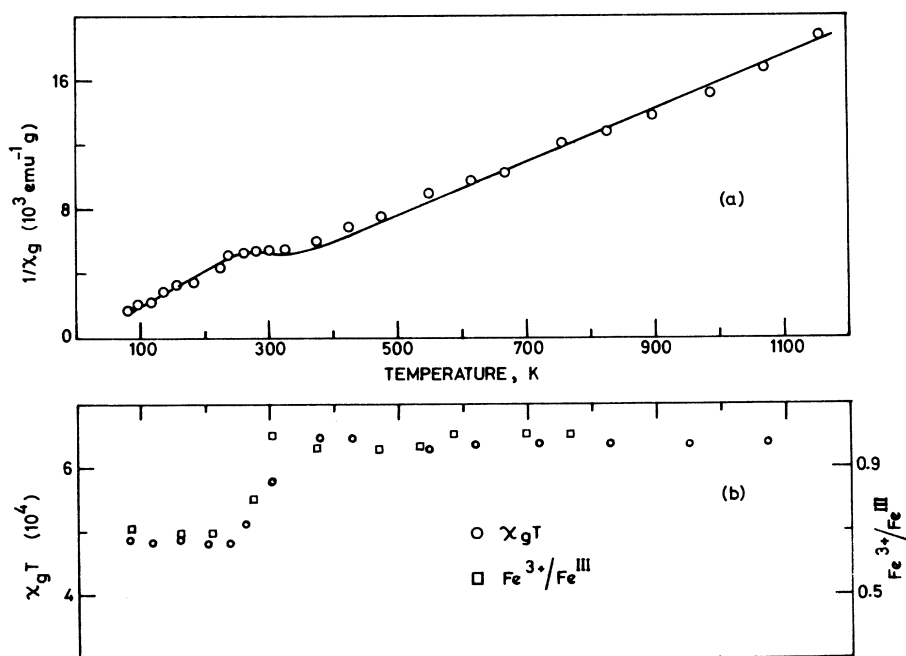


FIG. 2. (a) Plot of reciprocal susceptibility  $1/\chi_g$  vs temperature for  $\text{HoCoO}_3$  (sample I). (b) Plot of  $\chi_g T$  as a function of temperature for  $\text{HoCoO}_3$  (sample I). Also shown on the same figure is the variation of  $\text{Fe}^{3+}/\text{Fe}^{\text{III}}$  obtained from Mossbauer spectra.

the basis of low-spin-high-spin equilibria.<sup>5,6</sup> If one assumes the absence of any exchange interaction (for which evidence exists), we see from Eq. (1) that the variation of  $\chi_g T$  vs  $T$  should give the ratio of  $\text{Co}^{3+}/\text{Co(III)}$ . Such a variation is shown in Fig. 2(b). It is indeed very striking that the variation of  $\text{Co}^{3+}/\text{Co(III)}$  determined through magnetic-susceptibility measurements agrees remarkably close with that determined through Mössbauer studies [Fig. 2(b)]. This close correspondence clearly establishes that the relative populations of  $\text{Fe}^{3+}$  and  $\text{Fe(III)}$  determined from Mössbauer spectroscopy reflect the populations of  $\text{Co}^{3+}$  and  $\text{Co(III)}$  in  $\text{HoCoO}_3$ .

The ratio of  $\text{Fe}^{3+}$  to  $\text{Fe(III)}$  in  $\text{HoCoO}_3$  in the temperature range 78–200 K is lower than that in  $\text{LaCoO}_3$ .<sup>6</sup> Indeed the ratio increases in the following order:  $\text{HoCoO}_3 < \text{GdCoO}_3 < \text{LaCoO}_3$ .<sup>11</sup> This variation of the  $\text{Fe}^{3+}/\text{Fe(III)}$  ratio with the change in the rare-earth ion can be explained as follows. It has been observed earlier that the low-spin-high-spin equilibrium in rare-earth cobaltates depends upon the relative strength of the crystal-field splitting  $\Delta_{cf}$  and the exchange energy  $\Delta_{ex}$ . It is likely that the polarization of the ligand orbitals by the ions outside the coordination octahedron may have a significant perturbing influence on the crystal-field splitting  $\Delta_{cf}$  which in semicovalent oxides is determined to a first approximation by two opposing factors, namely, the formation of  $\sigma$  and  $\pi$  bonds.<sup>12–14</sup> The rare-earth cobaltates<sup>15</sup> (except for  $\text{LaCoO}_3$  which is rhombohedral) crystallize in the orthorhombic structure with the space group  $Pbnm$  which is a distorted perovskite. The crystallographic unit cell contains four equivalent cobalt ions. The distortion of the perovskite structure is such that the cobalt environment remains essentially octahedral; however, the axes of the four octahedral sites are in different directions. One can visualize the structure as a three-dimensional network of strings of oxygen octahedra whose axes zig-zag slightly. The degree of zig zagging of the octahedra is determined by the size of the rare-earth ion. The larger the rare-earth ion, the lesser is the zig zagging so that in  $\text{LaCoO}_3$  the Co-O-Co chains are almost linear. The Co-O-Co bond of  $\pi$  type which results from the overlapping of the  $t_{2g}$  orbitals by the  $p_r$  orbitals of oxygen enters into competition with the  $\sigma$  bond (rare-earth-O). The importance of this bond in perturbing the  $\sigma$  (Co-O) bond depends upon the acidity of the rare-earth ion, which decreases in the following order  $\text{Ho} > \text{Gd} > \text{La}$ . Consequently, the perturbing effect is more pronounced in  $\text{HoCoO}_3$  than in  $\text{GdCoO}_3$  which in turn is more than that in  $\text{LaCoO}_3$ . The net effect of this polarization of the ligand orbitals by the rare-earth ion is probably to increase  $\Delta_{cf}$  in the following order:  $\text{HoCoO}_3 > \text{GdCoO}_3 > \text{LaCoO}_3$ . This increase in

$\Delta_{cf}$  causes a decrease in the ratio of  $\text{Co}^{3+}/\text{Co(III)}$  as observed<sup>16</sup>:  $\text{LaCoO}_3 > \text{GdCoO}_3 > \text{HoCoO}_3$ . Although we have not been able to complete detailed investigations of other rare-earth cobaltates, our preliminary studies<sup>11</sup> do indicate that the ratio  $\text{Co}^{3+}/\text{Co(III)}$  decreases as the radius of the rare-earth ion decreases.

Such a change in  $\Delta_{cf}$  with the radius of the rare-earth ion would imply that the covalency of the Co-O bond in the rare-earth cobaltates would increase as the radius of the rare-earth ion increases. Fortunately, Mössbauer isomer-shift systematics gives an indication about the degree of covalency in the compound. It is interesting to mention that the isomer shift for  $\text{Fe}^{3+}$  resonance in  $\text{LaCoO}_3$  is 0.5 mm/sec,<sup>6</sup> whereas in  $\text{GdCoO}_3$ <sup>11</sup> and  $\text{HoCoO}_3$ , the isomer shifts are 0.57 mm/sec and 0.65 mm/sec, respectively (at 78 K). In general it is found that the isomer shift decreases as the radius of the rare-earth ion increases.

In  $\text{HoCoO}_3$ , the ratio of  $\text{Fe}^{3+}/\text{Fe(III)}$  remains roughly 0.7 up to 250 K. This ratio abruptly increases to 1.0 in the temperature range 250–300 K, that is, above 300 K,  $\text{Co}^{3+}$  and  $\text{Co(III)}$  are equally populated. In the orthorhombic structure of  $\text{HoCoO}_3$ , there are four equivalent cobalt sites and as we have mentioned the structure can indeed be considered as a three-dimensional array of zig-zagging oxygen octahedra containing cobalt ions. Since the radius of the  $\text{Co(III)}$  ion which has empty orbitals of  $e_g$  symmetry is significantly smaller than that of a  $\text{Co}^{3+}$  ion which has half-filled antibonding orbitals of  $e_g$  symmetry, the oxygen ions between two dissimilar cobalt ions become displaced towards the  $\text{Co(III)}$  ion and away from the  $\text{Co}^{3+}$  ions. Elastic energy arising out of this distortion is conserved by a correlation of only  $\text{Co(III)}$  ions as near neighbors of the high-spin  $\text{Co}^{3+}$  ions. As temperature increases, this correlation can only be realized by ordering of the  $\text{Co(III)}$  ions and  $\text{Co}^{3+}$  ions within alternate oxygen octahedra; the smaller oxygen octahedra containing  $\text{Co(III)}$  ions, whereas relatively extended octahedra contain the  $\text{Co}^{3+}$  ion. This long-range ordering will reflect itself in several ways. We have not been able to detect the ordering and the changes in Co-O distances by x-ray studies; however, the Lamb-Mössbauer factor, x-ray Debye-Waller factor, and magnetic-susceptibility studies do suggest some sort of ordering. The Lamb-Mössbauer factor which reflects the dynamics of Co ion increases appreciably within the temperature range 250–300 K, suggesting a better binding and an ordered structure. Although the x-ray Debye-Waller factor reflects the over-all binding of the lattice, it is seen that the Debye-Waller factor decreases [Fig. 3(a)] in this temperature range, again indicating better binding and an ordered structure.

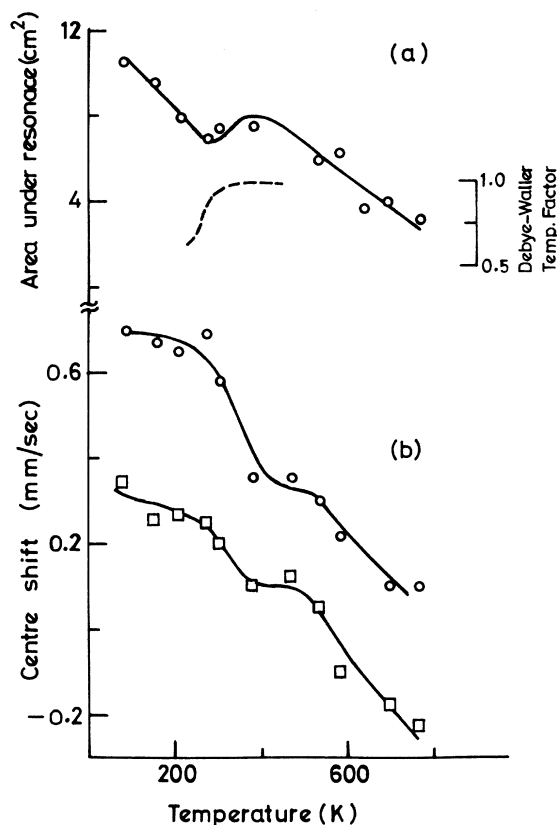


FIG. 3. (a) Variation of total area under resonance dips as a function of temperature, for  $\text{HoCoO}_3$  (sample I). Variation of x-ray Debye-Waller factor (dotted line) is also shown in this figure. (b) Variation of center shift for the two resonances of  $\text{HoCoO}_3$  (sample I) as a function of temperature.

Measurements on another sample of  $\text{HoCoO}_3$  heated only up to 980 K show a similar behavior except that the marked jump in  $\text{Fe}^{3+}/\text{Fe(III)}$  ratio occurs in a different temperature region ( $\sim 500$  K). In Fig. 4 we have shown the variation of  $\chi_g T$  and Lamb-Mössbauer factor with temperature for this sample. Since elastic energy consequent on the movement of oxygen ion towards  $\text{Co(III)}$  ions and away from  $\text{Co}^{3+}$  ions is the determining factor for ordering, it is natural to expect that the ordering temperature will be sensitive to sample preparation and treatment.

The ordering of low-spin  $\text{Co(III)}$  and high-spin  $\text{Co}^{3+}$  in alternate oxygen octahedra has another important effect on the overlap integrals  $\Delta_{\text{cac}}^{\sigma}$  and  $\Delta_{\text{cac}}^{\tau}$ . If  $N_{\sigma}$  and  $N_{\tau}$  are the normalization constants,  $\lambda_{\sigma}$  and  $\lambda_{\tau}$  are a measure of the covalent mixing of the cationic orbitals with anionic orbitals  $\varphi_{\sigma}$  and  $\varphi_{\tau}$ , and  $f_{\sigma}$  and  $f_{\tau}$  are the cationic orbitals of  $e_g$  and  $t_{2g}$  symmetry, then following Raccah and Goodenough<sup>5</sup> it can be shown that

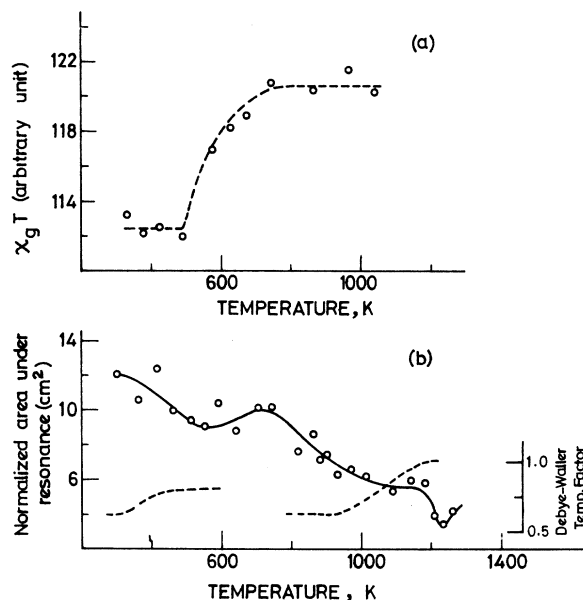


FIG. 4. (a) Plot of  $\chi_g T$  as a function of temperature for  $\text{HoCoO}_3$  (sample II). (b) Area under resonance dips as a function of temperature for  $\text{HoCoO}_3$  (sample II). Notice the transition around 1200 K is not shown in Fig. 3(a). X-ray Debye-Waller factor (dotted line) is also shown in the figure.

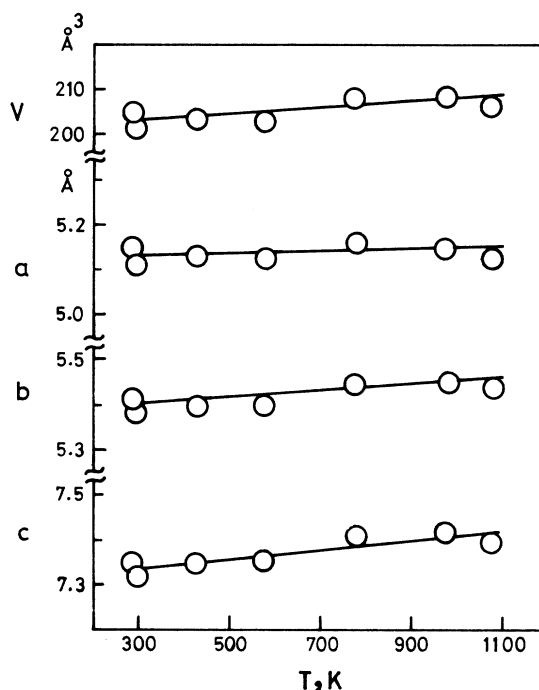


FIG. 5. Variation of lattice parameters and unit cell volume of orthorhombic  $\text{HoCoO}_3$  (sample I) with temperature.

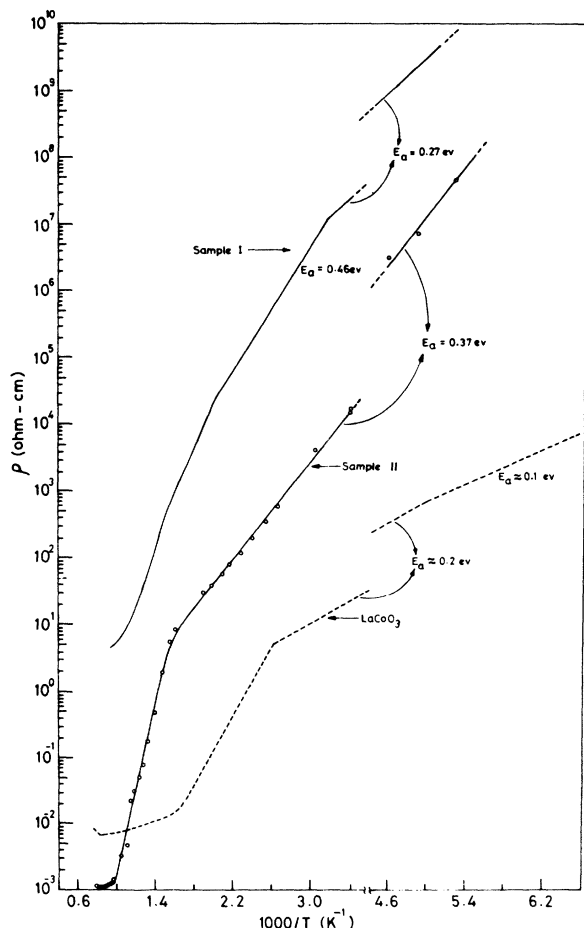


FIG. 6. Plot of logarithm of electrical resistivity vs reciprocal of absolute temperature for  $\text{HoCoO}_3$  (samples I and II). Data for  $\text{LaCoO}_3$  are given for purpose of comparison.

$$\Delta_{\text{cac}}^{\sigma} = N_{\sigma}^2 \lambda_{\sigma}^2,$$

$$\Delta_{\text{cac}}^{\tau} = N_{\tau}^2 [\lambda_{\tau}^2 + 2 \lambda_{\tau} (f_t, \varphi_{\tau})].$$

As the intervening oxygen ion moves towards the  $\text{Co(III)}$  ion and away from the  $\text{Co}^{3+}$  ion,  $\Delta_{\text{cac}}^{\sigma}$  becomes

$$\Delta_{\text{cac}}^{\sigma} = N_{\sigma}^2 (\lambda_{\sigma} + \gamma_1) (\lambda_{\sigma} - \gamma_{11}) > N_{\sigma}^2 \lambda_{\sigma}^2,$$

where  $(\lambda_{\sigma} + \gamma_1)$  is the mixing parameter for a low-spin  $\text{Co(III)}$  ion and  $(\lambda_{\sigma} - \gamma_{11})$  is the mixing parameter for a  $\text{Co}^{3+}$  ion. It therefore follows that as ordering takes place  $\Delta_{\text{cac}}^{\sigma}$  increases. The progressive increase in the overlap integral in this temperature range would initiate the delocalization of  $e_g$  electrons to form a  $\sigma^*$  band, with perhaps  $t_{2g}$  electrons still localized. This increase in the overlap integral is expected to be reflected in several ways. Because of this increase in the overlap integral, the Mössbauer isomer shift is expected to decrease in this temperature region. It is in-

teresting to note that the center shift [Fig. 3(b)] for both the resonances decreases appreciably in the ordering region (250–300 K for sample I). Obviously there may be various contributory factors for the observed changes in the center shift. These could be a (i) change in the second-order Doppler shift arising out of a change in  $\Theta_D$  at the transition temperature, (ii) change in the isomer shift because of the change in overlap integral, and (iii) abrupt change in the volume occurring at the transition temperature. The temperature dependence of the lattice parameters of orthorhombic  $\text{HoCoO}_3$  (Fig. 5) shows no abrupt volume change in the transition region. It does not, however, preclude the change in the volume of alternating oxygen octahedra still retaining more or less the original overall unit cell volume. The changes in  $\Theta_D$  at the transition temperature cannot account for the observed changes in the center shift. It appears, therefore, that the observed changes in the center shift may essentially be due to the changes in the isomer shift consequent on the increase in  $\Delta_{\text{cac}}^{\sigma}$  and  $\Delta_{\text{cac}}^{\tau}$ .

Another consequence of the increase in  $\Delta_{\text{cac}}^{\sigma}$  and  $\Delta_{\text{cac}}^{\tau}$  and the initiation of the delocalization of the  $e_g$  electrons to form the  $\sigma^*$  band is the change occurring in the resistivity temperature curve in this temperature region. The  $\log_{10} \rho$ -vs- $1/T$  plot (Figure 6) shows a break around the same temperature where we have found the susceptibility anomaly and the establishment of long-range order.<sup>17</sup> Similar

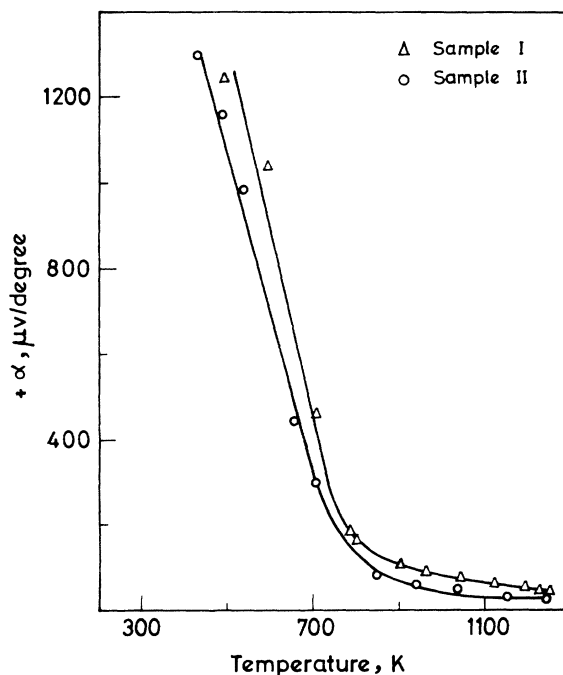


FIG. 7. Seebeck coefficient data on  $\text{HoCoO}_3$ .

changes in  $\log_{10}\rho - 1/T$  curves were observed in  $\text{LaCoO}_3$  in the ordering-temperature region. Beyond the ordering temperature, the resistivity decreases sharply until the substance becomes metallic around 1180 K. There is a first-order endothermic transition ( $\Delta H \sim \text{kcal mole}^{-1}$ ) around this temperature in the DTA curve and the Lamb-Mössbauer factor shows an abrupt increase (Fig. 4). We feel that the transition around 1180 K signifies a transition from localized electrons to itinerant electrons which is caused essentially by the large change in the entropy ( $\sim 2.5$  e. u.) of  $d$  electrons. An increase in the Lamb-Mössbauer factor indicates that the mean-square displacement of cobalt ions decreases sharply beyond the transition temperature.

Resistivity at low temperatures is considerably higher than that of  $\text{LaCoO}_3$ . As indicated earlier,

the Mössbauer isomer shift in this temperature region has indicated that  $\text{HoCoO}_3$  is less covalent than  $\text{GdCoO}_3$  which in turn is less covalent than  $\text{LaCoO}_3$ . Interestingly enough, the resistivity of the cobaltates decreases as the radius of the rare-earth ion increases:  $\text{LaCoO}_3 < \text{GdCoO}_3 < \text{HoCoO}_3$ . Further, because of less covalency, there is understandably no electron transfer from  $\text{Co}^{3+}$  to  $\text{Co(III)}$  in  $\text{HoCoO}_3$  as in the case of  $\text{LaCoO}_3$ . The absence of electron transfer from  $\text{Co}^{3+}$  to  $\text{Co(III)}$  to form  $\text{Co(II)}$  and  $\text{Co}^{4+}$  gives an excellent correlation between the ratio of  $\text{Co}^{3+}/\text{Co(III)}$  computed using susceptibility and Mössbauer data.

Seebeck coefficient data of  $\text{HoCoO}_3$  are similar to other cobaltates (Fig. 7). The material remains  $p$  type throughout the temperature range and attains a low and constant value at high temperatures indicating metal-like behavior.

- 
- <sup>1</sup>J. B. Goodenough, *Phys. Rev.* **164**, 789 (1968); *Czech. J. Phys.* **17B**, 304 (1967); *Prog. Solid State Chem.* **5**, 145 (1972).
- <sup>2</sup>C. N. R. Rao and G. V. Subba Rao, *Phys. Status Solidi* **1**, 597 (1970).
- <sup>3</sup>J. B. Goodenough and J. M. Longo, *Landolt-Bornstein Group III*, Vol. 4a, p. 131 (unpublished).
- <sup>4</sup>G. V. Subba Rao, B. M. Wanklyn, and C. N. R. Rao, *J. Phys. Chem. Solids* **32**, 345 (1971).
- <sup>5</sup>P. M. Raccach and J. B. Goodenough, *Phys. Rev.* **155**, 932 (1967).
- <sup>6</sup>V. G. Bhide, D. S. Rajoria, G. Rama Rao, and C. N. R. Rao, *Phys. Rev. B* **6**, 1021 (1972).
- <sup>7</sup>V. G. Bhide, D. S. Rajoria, Y. S. Reddy, G. Rama Rao, G. V. Subba Rao, and C. N. R. Rao, *Phys. Rev. Lett.* **28**, 1133 (1972).
- <sup>8</sup>P. K. Gallagher, *Mater. Res. Bull.* **3**, 225 (1968).
- <sup>9</sup>V. G. Bhide and M. S. Multani, *Phys. Rev.* **139**, A1983 (1965).
- <sup>10</sup>The effective magnetic moment (spin-only) of  $\text{Ho}^{3+}$  is  $10.5\mu_B$ .
- <sup>11</sup>V. G. Bhide, D. S. Rajoria, G. Rama Rao, and C. N. R. Rao (unpublished).
- <sup>12</sup>A. D. Liehr, *J. Phys. Chem.* **67**, 1314 (1963).
- <sup>13</sup>J. Fergusson, K. Knox, and D. L. Wood, *J. Chem. Phys.* **35**, 2236 (1961).
- <sup>14</sup>A. Casalot, P. Dougier, and P. Hagemuller, *J. Phys. Chem. Solids* **32**, 407 (1971).
- <sup>15</sup>A. Kappatsch, S. Quezel-Ambrunaz, and J. Sivardière, *J. Phys. (Paris)* **31**, 369 (1970).
- <sup>16</sup>Low-temperature resistivity data (78–250 K) of  $\text{HoCoO}_3$  show the activation energy for conduction,  $E_a$  ( $\rho = \rho_0 e^{-E_a/kT}$ ) to be  $\sim 0.3$  eV. This is much larger than the  $E_a$  value in  $\text{LaCoO}_3$  ( $\sim 0.1$  eV). In  $\text{LaCoO}_3$ , the energy difference between  $\text{Co}^{3+}$  and  $\text{Co(III)}$  is estimated to be  $\sim 0.05$  eV (Ref. 6).
- <sup>17</sup>These breaks are around 320 and 590 K in samples I and II, respectively. These correspond closely with our measurements of Lamb-Mössbauer factor, Debye-Waller factor, and susceptibility anomaly (see Figs. 2, 3, and 5). Slight decomposition is noted above 1200 K.